

Elsevier required licence: © <2021>. This manuscript version is made available under the CC-BY-NC-ND 4.0 license <http://creativecommons.org/licenses/by-nc-nd/4.0/>  
The definitive publisher version is available online at  
[<https://www.sciencedirect.com/science/article/pii/S0043135420310745?via%3Dihub>]

1 **Understanding the fate and impact of capsaicin in anaerobic co-digestion of**  
2 **food waste and waste activated sludge**

3 Mingting Du<sup>a,b</sup>, Xuran Liu<sup>a,b</sup>, Dongbo Wang<sup>a,b,\*</sup>, Qi Yang<sup>a,b</sup>, Abing Duan<sup>a,b,\*</sup>, Hong Chen<sup>c</sup>, Yiwen Liu<sup>d</sup>, Qilin

4 Wang<sup>d</sup>, Bing-Jie Ni<sup>d</sup>

5 <sup>a</sup> College of Environmental Science and Engineering, Hunan University, Changsha 410082, P.R. China

6 <sup>b</sup> Key Laboratory of Environmental Biology and Pollution Control (Hunan University), Ministry of Education,

7 Changsha 410082, P.R. China

8 <sup>c</sup> Key Laboratory of Water-Sediment Sciences and Water Disaster Prevention of Hunan Province, School of

9 Hydraulic Engineering, Changsha University of Science & Technology, Changsha 410004, China

10 <sup>d</sup> Centre for Technology in Water and Wastewater, School of Civil and Environmental Engineering, University

11 of Technology Sydney, Sydney, NSW 2007, Australia

12 First author: Mingting Du ([dumingting123@163.com](mailto:dumingting123@163.com))

13 Corresponding author: Dongbo Wang ([w.dongbo@yahoo.com](mailto:w.dongbo@yahoo.com)) and Abing Duan ([duanabing@hnu.edu.cn](mailto:duanabing@hnu.edu.cn))



## 14 ABSTRACT

15 Anaerobic co-digestion is an attractive option to treat food waste and waste activated sludge, which is  
16 increasingly applied in real-world situations. As an active component in *Capsicum* species being  
17 substantially present in food waste in many areas, capsaicin has been recently demonstrated to inhibit the  
18 anaerobic co-digestion. However, the interaction between capsaicin and anaerobic co-digestion are still  
19 poorly understood. This work therefore aims to deeply understand the fate and impact of capsaicin in the  
20 anaerobic co-digestion. Experiment results showed that capsaicin was completely degraded in anaerobic  
21 co-digestion by hydroxylation, O-demethylation, dehydrogenation and doubly oxidization, respectively.  
22 Although methane was proven to be produced from capsaicin degradation, the increase in capsaicin  
23 concentration resulted in decrease in methane yield from the anaerobic co-digestion. With an increase of  
24 capsaicin from  $2 \pm 0.7$  to  $68 \pm 4$  mg/g volatile solids (VS), the maximal methane yield decreased from  $274.6 \pm$   
25  $9.7$  to  $188.9 \pm 8.4$  mL/g VS. The mechanic investigations demonstrated that the presence of capsaicin  
26 induced apoptosis, probably by either altering key kinases or decreasing the intracellular  $\text{NAD}^+/\text{NADH}$  ratio,  
27 which led to significant inhibitions to hydrolysis, acidogenesis, and methanogenesis, especially acetotrophic  
28 methanogenesis. Illumina Miseq sequencing analysis exhibited that capsaicin promoted the populations of  
29 complex organic degradation microbes such as *Escherichia-Shigella* and *Fonticella* but decreased the  
30 numbers of anaerobes relevant to hydrolysis, acidogenesis, and methanogenesis such as *Bacteroides* and  
31 *Methanobacterium*.

32 **Keywords:** Capsaicin; Food waste; Waste activate sludge; Anaerobic co-digestion; Methane production

## 33 1. Introduction

34 Food waste (FW) and waste activated sludge (WAS) are two major bio-solids in the world, which are  
35 massively generated. It is documented that more than 1.3 billion tons FW are globally produced each year

36 (Li et al. 2020b, Xu et al. 2018), and the annual amount is estimated to achieve approximately 2.2 billion tons  
37 by 2025 (Mehariya et al. 2018). In China, more than 90 million tons of FW is produced each year,  
38 accounting for 37-62 % of municipal solid waste (Zhang et al. 2014). As for WAS, its amount in China is  
39 over 40 million tons per year, and increases at an annual average rate of 4.75 % (Luo et al. 2020b). The total  
40 amount in the world is estimated to increase to 103 million tons by 2025 (Yao et al. 2018).

41 FW and WAS contain substantial degradable substrates (e.g., proteins, carbohydrates, and lipids) and also  
42 several recalcitrant or toxic materials such as cellulose, humus antioxidant, antibiotic, and heavy metals (Liu  
43 et al. 2020a, Shah et al. 2005, Tao et al. 2020, Wang et al. 2019a). They will pose high risks to the  
44 environment if they are not treated appropriately (Li et al. 2020a). As a mature technology to effectively  
45 prevent pollution and recover energy concurrently, anaerobic digestion attracts much attention (Liu et al.  
46 2020b, Luo et al. 2020a). Compared with the mono-digestion, anaerobic co-digestion of FW and WAS offers  
47 complementary benefits such as substrate variability, toxicity dilution, and C/N ratio balance (Sole-Bundo et  
48 al. 2017, Zhao et al. 2016). Therefore, it has been recently thought to be a very promising option and  
49 growingly executed in field situations (Nghiem et al. 2017).

50 Capsaicin, a major pungent ingredient in varieties of capsicums, is widely used as food additives  
51 throughout the world, especially in South East Asian, Latin-American countries and southwest of China  
52 (Kurita et al. 2002, Surh and Lee 1995). For instance, the daily consumption of capsicum spices is 5  
53 g/person in Thailand (Monseeranusorn 1983) and 20 g/person (one chili pepper) in Mexico (López-Carrillo et  
54 al. 1994). The capsaicin content in capsicums usually ranges from 0.1 to 2.5 mg/g (Parrish 1996). This  
55 indicates that capsaicin accumulation in FW could be up to 25 g/kg.

56 It is known that capsaicin has a wide variety of antimicrobial effects and can interact at primary sensory  
57 neurons exerting the characteristic actions of excitation, desensitization and neurotoxicity (Kurita et al. 2002).

58 Due to this characteristic, several efforts have been carried out to assess the toxicity of capsaicin to  
59 microorganisms. [Gu et al. \(2019\)](#) showed that the minimum inhibitory concentrations of capsaicin on  
60 *Streptococcus mutans*, *Actinomyces viscosus*, *Lactobacillus*, and *Streptococcus sanguis* were 50, 50, 50, 25  
61  $\mu\text{g/mL}$  respectively.

62 As anaerobic co-digestion is a biological process with varieties of anaerobes being involved, the presence  
63 of capsaicin might also affect these microbes. [Li et al. \(2016\)](#) demonstrated that when the pungency degree  
64 decreased from 1136.1 to 71.5 Scoville Heat Units (i.e., 11.1 to 0.7 g Capsaicin/kg Kitchen Waste), the  
65 maximum methane production increased from 9.9 to 13.5 mL/ (g VS h), indicating the detrimental impact of  
66 capsaicin on anaerobic digestion. [Yue et al. \(2020\)](#) recently found that N-Vanillynonanamide (one type of  
67 capsaicin) inhibited anaerobic digestion of glycerol trioleate severely. As N-Vanillynonanamide addition  
68 increased from 0 to 40% wt, the methane yield decreased from 780.21 to 142.1 mL/g Total Volatile Solid.  
69 The findings obtained by the previous investigations confirmed the detrimental effect of capsaicin and raised  
70 our concerns in terms of the toxicity of capsaicin to anaerobic co-digestion. Considering the massive  
71 quantities of capsaicin-rich wastes treated daily, comprehensive and deep understanding the fate and impact of  
72 capsaicin in anaerobic co-digestion is of significance to manipulate the co-digesters in field situations.

73 Despite the excellent work made by Li et al. and Yue et al., details of what happen in capsaicin-rich  
74 co-digestion systems remain largely unknown. For example, capsaicin as an organic, it is unclear about the  
75 transformation and metabolism of capsaicin in the process of anaerobic co-digestion and its interaction with  
76 anaerobes. The contribution of capsaicin degradation to methane yield is also not clear. Moreover, as  
77 anaerobic co-digestion contains several processes such as disintegration, hydrolysis, acidogenesis,  
78 acetogenesis, and methanogenesis, it is also unknown that the mechanism of capsaicin effects on each process.

79 By clarifying these questions, this work aims to deeply understand the fate and impact of capsaicin in

80 anaerobic co-digestion of FW and WAS. Firstly, the fate of capsaicin in the co-digesters was systematically  
81 assessed. Then, the influence of capsaicin at different concentrations on methane production was  
82 investigated. Finally, details of how capsaicin affects methane production were explored. To our  
83 knowledge, this is the first study revealing the interaction between capsaicin and anaerobic co-digestion.

## 84 **2. Materials and methods**

### 85 **2.1 Source and characteristics of FW, WAS, and inocula.**

86 FW used in this work, which was mainly composed of rice, noodles, and vegetables, was withdrawn  
87 from a cafeteria in Hunan University (Changsha, China). The indigestible substrates (e.g., inorganic  
88 particles, bones, and chopsticks) were first removed before FW was crushed into small particles (1-3 mm) for  
89 further use. The main characteristics of FW are as follows: pH  $5.8 \pm 0.1$ , total solids (TS)  $121.3 \pm 5.8$  g/L,  
90 volatile solids (VS)  $116.1 \pm 4.3$  g/L, total chemical oxygen demand (TCOD)  $142.3 \pm 7.4$  g/L, total proteins  
91  $31.2 \pm 1.4$  g COD/L, total carbohydrates  $123.5 \pm 5.7$  g COD/L, and capsaicin content  $4 \pm 1$  mg/g FW. In this  
92 study, extra capsaicin, with purity being  $> 98\%$ , was purchased from Hefei Bomei Biotechnology company.

93 WAS used in this work was taken from the secondary tank of a municipal wastewater treatment plant in  
94 Changsha, China. WAS was first filtered with a  $2 \text{ mm} \times 2 \text{ mm}$  screen and then concentrated in  $4 \text{ }^\circ\text{C}$   
95 refrigerator for 24 h before use, and the main characteristics of WAS are as follows: pH  $6.9 \pm 0.1$ , TS  $57.3 \pm$   
96  $2.6$  g/L, VS  $28.3 \pm 1.2$  g/L, TCOD  $36.2 \pm 1.6$  g/L, total proteins  $8.5 \pm 0.3$  g COD/L, and total carbohydrates  
97  $1.6 \pm 0.1$  COD/L.

98 Inocula applied in this work were harvested from a mesophilic anaerobic reactor in our laboratory, which  
99 has been operated 130 days with solid retention time of 30 d and WAS as substrate. The main properties of  
100 inoculated sludge are as follows: pH  $7.2 \pm 0.1$ , TS  $46.7 \pm 3.5$  g/L, and VS  $38.6 \pm 2.3$  g/L.

### 101 **2.2 Effect of capsaicin on methane production from anaerobic co-digestion.**

102 This batch test was performed in six identical serum bottles, and the working volume of each bottle was  
103 500 mL. Among them, one was set as the blank, and the other five were operated as the experimental  
104 reactors. According to the literature, the mixture ratio of FW to WAS used in this study was set as 1:1 on a  
105 VS basis (Mehariya et al. 2018). Firstly, 1.5 L mixture of FW and WAS was evenly divided into the five  
106 experimental reactors, respectively. Then, different amounts of extra capsaicin were added into the reactors,  
107 which led to the initial capsaicin content of  $2 \pm 0.7$ ,  $8 \pm 1.2$ ,  $20 \pm 2.3$ ,  $36 \pm 2.6$ , or  $68 \pm 4.1$  mg/g VS. It  
108 should be emphasized that no extra capsaicin was added into the first experimental reactor, and  $2 \pm 0.7$  mg/g  
109 VS was the background value in the digestion mixture. To improve the uniformity of capsaicin, all the  
110 mixtures were pretreated in a water-bath shaker (120 rpm, 60 °C) for 30 min (Huang et al. 2020). When the  
111 mixtures were cooled down to room temperature, each reactor received 50 mL same inocula, as mentioned  
112 above. The blank reactor, which merely contained 50 mL inocula and 300 mL of Milli-Q water, was also  
113 conducted to test the methane productivity from the inocula alone. All the reactors were flushed with high  
114 purity nitrogen for 5 min to eliminate oxygen, sealed with rubber stoppers, and placed in an air-bath shaker  
115 (120 rpm) at  $35 \pm 1^\circ\text{C}$  for 45 d. pH value in all the reactors was maintained at  $7.0 \pm 0.1$  during the whole  
116 digestion period by 4 M hydrochloric acid or 4 M sodium hydroxide with automatic titrators.

117 In this work, all the tests, unless otherwise described, were operated in triplicate. The data reported  
118 below are net values, with the values determined in the blank reactor having been subtracted. During the  
119 entire digestion process, the yield of methane produced was determined periodically by releasing the pressure  
120 in the serum bottle using a 300 mL glass syringe to equilibrate with the room pressure according to the  
121 method documented in the literature (Liu et al. 2019), and the calculation of the cumulative volume of  
122 methane was detailed in our previous publication (Wang et al. 2015).

### 123 **2.3 Methane production from capsaicin.**

124 Three replicates serum bottles with a working volume of 500 mL each were carried out to assess whether  
125 capsaicin can be served as substrates to produce methane in the anaerobic co-digestion process. Each reactor  
126 received 50 mL same inocula. Among them, one bottle receives 300 mL of Milli-Q water and was set as the  
127 control, the other two bottles received 300 mL synthetic medium containing either 36 mg capsaicin/g VS or 68  
128 mg capsaicin/g VS as the extra digested substrate. All the operations were the same as depicted in Section  
129 2.2.

#### 130 **2.4 Effect of capsaicin on solubilization, hydrolysis, acidogenesis, and methanogenesis.**

131 This batch test was performed to assess the effect of capsaicin on digestion steps (i.e., solubilization,  
132 hydrolysis, acidogenesis, acetoclastic methanogenesis and hydrogenotrophic methanogenesis) relevant to  
133 methane production. The effect of capsaicin on WAS solubilization was assessed in real WAS by comparing  
134 the variations in soluble proteins and soluble polysaccharides in the presence of different capsaicin  
135 concentrations, while the impact of capsaicin on other biological processes was evaluated in synthetic media  
136 through comparing the specific degradation rates of the model substrates under different concentrations of  
137 capsaicin according to the previous study (Wu et al. 2019). In this test, fifteen replicate serum bottles were  
138 performed and divided into five groups (namely Test-I, Test-II, Test-III, Test-IV, and Test-V) with three in  
139 each.

140 Test-I: Three reactors with a working volume of 500 mL each were operated. The three reactors first  
141 received 300 mL mixture of FW and WAS, which capsaicin concentrations were  $2 \pm 0.7$ ,  $8 \pm 1.2$ ,  $36 \pm 2.6$   
142 mg/g VS, respectively. After being pretreated at 60 °C for 30 min, each reactor was fed with 50 mL inocula.  
143 All other conditions were the same as those described above. By measuring the concentrations of soluble  
144 proteins and carbohydrates in the initial 2 days, the effect of capsaicin on solubilization could be obtained.

145 Test-II: Three replicate anaerobic digestion reactors were operated. Each reactor received 50 mL

146 identical inocula and 300 mL same synthetic wastewater containing 5.3 g dextran. In the anaerobic  
147 co-digestion of this study, carbohydrates are the dominate substrate used for hydrolysis, and the carbohydrates  
148 in synthetic wastewater were similar to that in the co-digestion substrate. Afterwards, 0, 11 and 18 mg  
149 capsaicin were respectively added into the three reactors, which resulted in the initial capsaicin condition of 0,  
150 30 and 50 mg/L, respectively. All other conditions were the same as those described above. By measuring  
151 the specific degradation rate of dextran, the effect of capsaicin on hydrolysis process could be indicated.

152 Test-III: This test was operated the same as described in Test-II except that the substrate (i.e., dextran) in  
153 synthetic wastewater was replaced by 2.7 g glucose, respectively.

154 Text-IV: The operation of this test was performed with the same approach as described in Test-II except  
155 that 1.25 g sodium acetate was employed to replace dextran in synthetic wastewater.

156 Test-V: In this test, three reactors were operated. Each received 50 mL identical inocula and 300 mL  
157 Milli-Q water containing 0, 11 or 18 mg capsaicin. Afterwards, each reactor was flushed with a mixed gas  
158 (40% hydrogen, 10% carbon dioxide and 50% nitrogen) for 5 min to ensure that each was full of synthetic  
159 hydrogen-containing gas. At last, all these reactors were capped with rubber stoppers, sealed, and placed in  
160 an incubator (120 rpm) at  $35 \pm 1^\circ\text{C}$ .

## 161 2.5 Model-based Analysis.

162 Methane production was simulated by the modified Gompertz equation (Eq(1)) (Lay et al. 1997), and  
163 several kinetic parameters, e.g.,  $Mm$  (maximum methsane yield potential, mL/g VS or mL/L),  $Rm$  (methane  
164 production rate, mL/(g VS·d) or mL/d or mL/(L·d)),  $\lambda$  (lag phase time of methane production, d), and  $t$   
165 (digestion time, d) were calculated using Origin 7.0 software.

$$166 \quad \text{—————} \quad (1)$$

167 The effect of capsaicin on each process of anaerobic co-digestion can be assessed by the inhibition

168 constant, which is obtained from Eq (2).

169 (2)

170 Where,  $X$  is the reaction rate, subindex “s” is the substrate, subindex “i” is the inhibitor,  $I_i$  is the  
171 concentration of inhibitor (mg/L), and  $K_{s,i}$  is the relevant inhibition constant (mg/L).

## 172 **2.6 Analytical Methods.**

173 The analyses of Total Suspended Solid (TSS), Volatile Suspended Solid (VSS), TCOD, and SCOD were  
174 conducted in accordance with Standard Methods. Carbohydrate was measured by phenol-sulfuric method  
175 with glucose as the standard. Protein was determined by the Lowry-Folin method with BSA as the standard.  
176 The composition in biogas was analyzed by gas chromatograph equipped with a thermal conductivity detector  
177 according to the method documented in the literature ([Wang et al. 2019b](#)).

178 The concentration of capsaicin was determined using HPLC according to the reference ([Hwang et al.](#)  
179 [2017](#)). The samples were first centrifuged at 6500 rpm at 4 °C for 10 min and dried at 58 °C for 48 h by  
180 Vacuum drying oven. Then, 0.2 g dried sample was weighed and dissolved in n-hexane. The dissolved  
181 sample was shocked for 5 min before being placed into ultrasonic machine for 10 min. After the sample was  
182 re-centrifuged at 2500 rpm for 5min, the normal hexane extract was filtered through 0.22 µm filterable  
183 membrane and then injected into HPLC system (Agilent 1200, USA). The mobile phase was methyl alcohol  
184 and deionized water (70:30, v/v) with a flow rate 1.0 mL/min. The absorbance was measured at 280 nm.

185 The major metabolic products of capsaicin in the digestion process were measured via liquid  
186 chromatography-mass spectrometer/mass spectrometer ([Jia et al. 2018](#)). The metabolic products were  
187 extracted using solid phase NH<sub>2</sub> Cartridge (6 mL, 500 mg sorbent) and then eluted with methanol. The  
188 eluant was filtered through 0.22 µm filterable membrane and injected into LC-MS/MS (LC-MS/MS, Agilent  
189 1290 series LC, 6460 Triple Quad LC/MS). The metabolic products were separated using a ZORBAX

190 RRHD Eclipse Plus C18 column (2.1 × 50mm, 1.8 μm) and the mass spectrometers were performed in  
191 positive electron-spray ionization (ESI+) mode. The samples preparation and determination method of  
192 LC-MS/MS were detailed in Supplementary Information (SI).

193 For determining the activity of key enzymes, 25 mL sample was taken out from the reactors, cleaned  
194 using 100 mM sodium phosphate buffer (pH 7.4), sonicated at 20 kHz at 4 °C for 10 min, and finally  
195 centrifuged at 12000 rpm at 4 °C for 15 min to remove the debris. The extracts were kept on the ice before  
196 analyzing. The relative activities of function enzymes (mch, F420, AK, PTA, Coenzyme A, acetyl-CoA  
197 decarboxylase/synthase complex (ACDS) and Coenzyme M) relevant to methane production were analyzed  
198 using previously reported methods (Grahame and DeMoll 1996, Li et al. 2015, Liu et al. 2015, Wang et al.  
199 2018a).

200 The membrane fluidity of microbial cells was determined by flow cytometry using Annexin V-FITC  
201 fluorescence dye according to the reference (Luo et al. 2016). Briefly, the samples were centrifuged in a 50  
202 mL tube at 6000 rpm for 5 min, with the pellet being suspended by pre-cooled phosphate buffer saline (PBS).  
203 Then the suspension was heated at 60 °C in a water bath for 30 min and re-suspended by pre-cooled PBS.  
204 After filtering the suspension using 500 Nylon mesh and stained, the samples were determined using BD  
205 Biosciences AccuriC6 flow cytometer (Bacton Dickinson Immunocytometry Systems, San Jose, CA, USA),  
206 with the staining process being available in SI.

207 For microbial community analysis, the collected samples were first centrifuged for 5 min at 10000 rpm.  
208 Then, the total DNA was extracted from the samples using the Fast DNA kit (MoBio Laboratories) according  
209 to the instruction from manufacture. The quantity and purity of DNA were analyzed with a Nanodrop  
210 spectrophotometer (Thermo Scientific, Wilmington, DE, USA). The high-throughput sequencing (Illumina  
211 Miseq) was conducted by Majorbio co., Ltd. (Shanghai, China). The primers 515F

212 (5'-GTGCCAGCMGCCGCGG-3') and 806R (5'-GGACTACHVGGGTWTCTAAT-3') targeting the V4  
213 regions of bacterial 16S DNA genes were used.

## 214 **2.7 Statistical Analysis.**

215 All the batch experiments were performed in triplicate. An analysis of variance (ANOVA) with least  
216 significant difference test was used to assess the significance of results, and  $p < 0.05$  was considered  
217 statistically significant.

## 218 **3. Results and discussion**

### 219 **3.1 Capsaicin variation in anaerobic co-digestion.**

220 Fig. 1A shows the variations in HPLC chromatogram of extracted mixtures taken from the reactor fed  
221 with  $68 \pm 4.1$  mg/g VS capsaicin at different digestion times. According to HPLC chromatogram tested with  
222 the standard capsaicin, the absorption peak of capsaicin appears at near 4.5 min (Fig. S1). It can be seen that  
223 the absorption peak gradually declined with the digestion time, which indicates that capsaicin was degraded in  
224 the anaerobic co-digestion process. Quantitative calculation exhibits that the concentration of capsaicin in  
225 digestion mixture also decreased with the digestion. With the digestion time increase from 0 to 9 d,  
226 capsaicin concentration decreased from  $68 \pm 4.1$  to  $14.2 \pm 2.4$  mg/g VS. On 12 d digestion, less than 1 mg/g  
227 VS capsaicin was measured in the system, suggesting that capsaicin was almost degraded in the co-digestion  
228 completely. The results further suggests that the specific degradation rate of capsaicin in this co-digestion  
229 system is  $4.1$  mg/(g VS)·d. Similar observations were also made on other reactors fed with other capsaicin  
230 levels.

231 It is reported that capsaicin could be metabolized by crude enzyme preparations from body, midgut and  
232 Malpighian tubule of *Helicoverpa armigera* and *H. assulta* (Zhu et al. 2020). Through a CO<sub>2</sub> Evolution Test,  
233 Wang et al. (2014) demonstrated that capsaicin could be biodegraded by microbes and bio-converted to CO<sub>2</sub>

234 and H<sub>2</sub>O under aerobic conditions. When a filamentous fungus i.e., *Aspergillus oryzae*, was incubated with  
235 red pepper powder in potato dextrose broth, Lee et al. (2015a) found that capsaicin was degraded with five  
236 metabolites being obtained. Despite these significant researches, this is the first study proving the  
237 degradation of capsaicin in anaerobic co-digestion of FW and WAS.

### 238 3.2 Identification of the Main Metabolites of Capsaicin Degradation.

239 LC-MS/MS was used to identify the metabolites of capsaicin in anaerobic co-digestion process. Since  
240 the fragment ions of MS/MS spectrometry occurred at 10.496 min are the same to those produced from  
241 standard capsaicin (Fig. S2), the peak occurred at 10.496 min is considered to be capsaicin. On 0 d, one peak  
242 was detected at 10.496 min (M) in LC/MS chromatogram extracted the sample withdrawn from the digester  
243 fed with  $68 \pm 4.1$  mg/g VS. On 9 d, this peak decreased largely, and meanwhile three new peaks occurred,  
244 with their retention time being 6.708 min (M1), 8.362 min (M2), and 12.331 min (M3), respectively (Fig. 2).  
245 This confirms again that capsaicin was degraded in the anaerobic co-digestion and suggests that three major  
246 metabolic products were generated from capsaicin degradation. The proposed structure and details of  
247 metabolites are shown in Table S1.

248 To understand capsaicin biodegradation and identify these three metabolites, the precursor ions  $[M + H]^+$ ,  
249  $[M1 + H]^+$ ,  $[M2 + H]^+$ ,  $[M3 + H]^+$ , and their fragmentation patterns were further determined. The  
250 precursor ion peak of  $[M + H]^+$  at  $m/z$  306 indicates that the molecular weight of capsaicin was 305 (Fig. 3A).  
251 Besides, three fragment ions at  $m/z$  137, 170, and 182 were also found in Fig. 3A. The fragment ion at  $m/z$   
252 137 was reported to be vanillyl portion of capsaicin resulting from cleavage of C7-N8, while the product ions  
253 at  $m/z$  170 and 182 were respectively derived from fragmentation of alkyl chain at C7-N8 and C1-C7 (Reilly  
254 et al. 2003).

255 Analogous to capsaicin (M), the molecular weight of M1 was 321 due to the precursor ion peak of  
256  $[M1+H]^+$  at  $m/z$  322 (Fig. 3B). Apart from the precursor ion peak, there are other four fragment ions being  
257 observed in Fig. 3B. The presence of fragment ion at  $m/z$  137 indicated that vanilloid ring of capsaicin was  
258 not modified. Shifts in the product ions at  $m/z$  from 182 and 170 to 198 and 186 may be owing to addition of  
259 oxygen atom (16 amu) to the alkyl chain. The product ion at  $m/z$  181 was likely due to loss of hydroxyl  
260 group from fragment ion at  $m/z$  198 while the appearance of fragment ion at  $m/z$  304 was probably due to loss  
261 of terminal  $CH_2O$  from  $m/z$  322. Based on these analyses, M1 ( $m/z$  322) was inferred to alkyl hydroxylated  
262 metabolite of capsaicin, with its molecular structure being detailed in Fig. 3B. It was reported that the alkyl  
263 side chain of capsaicin was susceptible to enzymatic oxidation (Reilly and Yost 2006), and M1 was also  
264 detected as a capsaicin metabolite by *Aspergillus oryzae* (Lee et al. 2015a).

265 Four fragment ions were observed in the MS/MS spectrum of M2 (Fig. 3C). The precursor ion peak at  
266  $m/z$  292  $[M2+H]^+$  indicated that the molecular weight of M2 was 291. The appearance of fragment ion at  
267  $m/z$  123 was probably owing to a net loss of 14 amu from the vanilloid ring ( $m/z$  137) through demethylation  
268 of methoxy group. Gonzalez-Gil et al. (2019) demonstrated that tramadol and trimethoprim can transformed  
269 to O-desmethyltramadol and 4-desmethyltrimethoprim by demethylation of methoxy groups in anaerobic  
270 digestion. The existences of fragment ions at  $m/z$  170 and 182, however, suggested that the alkyl chain was  
271 not modified. Therefore, M2 was inferred to be an O-demethylation metabolite of capsaicin, which was  
272 previously detected in capsaicin degradation catalyzed by P450 enzyme as well (Reilly et al. 2003).

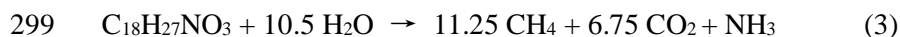
273 The precursor ion peak at  $m/z$  336  $[M3+H]^+$  indicated the molecular weight of M3 being 335 (Fig. 3D),  
274 which was 30 amu larger than that of capsaicin. It can be seen that the fragment ion at  $m/z$  170 still existed,  
275 suggesting that the alkyl chain at C7-N8 was unchanged. However, the fragment ion at  $m/z$  137 disappeared,  
276 which suggested that the vanilloid portion of capsaicin was modified. Two new fragment ions at  $m/z$  184

277 and 140 were detected. The fragment ion at m/z 184 was likely produced by cleavage of alkyl chain at  
278 N8-C9 of capsaicin, while the fragment ion at m/z 140 may be due to loss of -CH<sub>2</sub>NO from the fragment ion  
279 m/z 184. Thus, M3 was probably a doubly oxidized metabolite of dehydrogenated capsaicin, and this was  
280 also determined in capsaicin bioconversion by *H. armigera* (Tian et al. 2019).

### 281 3.3 Could methane be produced from capsaicin degradation?

282 The analyses above showed that in anaerobic co-digestion, capsaicin was first degraded into M1, M2,  
283 and M3 by hydroxylation, O-demethylation, dehydrogenation and doubly oxidization, respectively.  
284 According to the literature, these three metabolites would be further hydrolyzed into amino and carboxyl  
285 compounds by amidases, with the possible degradation pathway of capsaicin being proposed in Fig. 4 (Cho et  
286 al. 2014, Wang et al. 2018, Yue et al. 2020). However, it remains unknown whether these metabolic  
287 hydrolysates could be used for methane production in anaerobic co-digestion, requiring to be further clarified.

288 To figure out this possibility, one batch test was operated using either inocula or inocula + capsaicin as  
289 the digestion substrate, with the experimental details being shown in Section 2.3. It was found that about  
290 31.0 ± 0.9 mL methane was produced from the sole inocula whereas the corresponding value was 44.3 ± 1.3  
291 mL from inocula + 36 mg capsaicin/g VS and 59.9 ± 1.8 mL from inocula + 68 mg capsaicin/g VS (Fig. S3).  
292 This indicates that capsaicin could be served as substrate for methane production in anaerobic digestion.  
293 According to Eq (3), it can be calculated that 0.59 g (or 826 mL) of methane will be produced from 1 g  
294 capsaicin if it is completely digested, suggesting that 60 and 87 mL methane should be generated from inocula  
295 + 36 mg capsaicin/g VS and inocula + 68 mg capsaicin/g VS, respectively. However, the measured data  
296 from the two inocula + capsaicin digesters were much lower than the theoretical values. The possible  
297 reasons might be due to 1) incomplete utilization of capsaicin degradation intermediates and 2) inhibition of  
298 capsaicin to the activity of inocula.



### 300 **3.4 Effect of capsaicin on methane production.**

301 The cumulative methane yield during anaerobic co-digestion in the presence of capsaicin at different  
302 concentrations is shown in Fig. 5. It can be observed that methane yield in the reactor without extra  
303 capsaicin addition (i.e.,  $2 \pm 0.7$  mg/g VS capsaicin reactor) increased with the digestion time from 1 to 34 d,  
304 and no significant increase was observed after that day 34 ( $p > 0.05$ ). The optimum digestion time for this  
305 reactor was therefore 34 d, with the maximum methane yield of  $274.6 \pm 9.7$  mL/g of VS being measured.  
306 From Fig. 5, it was also found the increase of capsaicin affected methane production obviously. With an  
307 increase of capsaicin concentration from  $2 \pm 0.7$  to  $68 \pm 4.1$  mg/g VS, methane yield decreased from  $274.6 \pm$   
308  $9.7$  to  $188.9 \pm 8.4$  mL/g VS. Apart from methane yield, the optimum digestion time was also affected by  
309 capsaicin. For example,  $68 \pm 4.1$  mg/g VS of capsaicin increased the optimum digestion time to 58 d.

310 To further understand the effect of capsaicin on anaerobic digestion from the aspect of model, the  
311 modified Gompertz equation was employed to estimate three kinetic parameters, i.e., maximum methane yield  
312 potential ( $Mm$ ), methane production rate ( $Rm$ ), and lag phase time ( $\lambda$ ). It can be found that the Gompertz  
313 equation described the experimental data well, with  $R^2 > 0.99$  in all the scenarios (Fig. 5). When capsaicin  
314 concentration increased from  $2 \pm 0.7$  to  $68 \pm 4.1$  mg/g VS, the determined  $Mm$  and  $Rm$  decreased respectively  
315 from  $257.4$  mL/g VS and  $17.8$  mL/(g VS·d) to  $189.9$  mL/g VS and  $6.6$  mL/(g VS·d), whereas the calculated  $\lambda$   
316 increased from  $6.7$  to  $14.7$  d. This indicates that the increase of capsaicin not only decreased biochemical  
317 methane potential but also inhibited the rate of methane production.

318 According to the analyses above, it was demonstrated that the addition of capsaicin reduced rather than  
319 improved methane yield, though the addition of capsaicin provided extra substrate for anaerobes to produce  
320 methane. This suggests that anaerobic co-digestion from original substrates was largely inhibited by

321 capsaicin, which was in accordance with the results reported previously (Yue et al. 2020). Based on the  
322 experimental data obtained in the current work, it was estimated that 50% inhibitory concentration of  
323 capsaicin to anaerobic co-digestion was around 36.26 mg capsaicin/g VS (Fig. S4). Since anaerobic  
324 co-digestion includes several processes such as solubilization, hydrolysis, acidogenesis, and methanogenesis,  
325 the mechanism of how capsaicin affects methane production were explored in the following text.

### 326 **3.5 Mechanism of How Capsaicin Inhibits Anaerobic Co-digestion.**

327 It was found that the concentrations of soluble proteins and carbohydrates increased with capsaicin  
328 concentration (Fig. 6A and Fig. 6B). For example, the concentrations of soluble proteins and carbohydrates  
329 in the reactor fed with  $2 \pm 0.7$  mg/g VS capsaicin were respectively  $882.7 \pm 23.2$  and  $2695.4 \pm 25.5$  mg  
330 COD/L, while the corresponding concentrations in the reactor fed with  $68 \pm 4.1$  mg/g VS capsaicin were  
331  $1505.8 \pm 29.1$  and  $5530.2 \pm 53.2$  mg COD/L, respectively. According to the literature, an increase in the  
332 fluorescence intensity indicates an increase in soluble organics in digestion liquid (Fig. 6C) (Xu et al. 2017).  
333 There are two peaks, which are respectively located at Ex/Em of 200-250/290-320 and 250-280/<380 nm,  
334 being found in all the samples (Fig. 6C). The fluorescence intensity of both the peaks increased with the  
335 addition of capsaicin, suggesting that an increase of capsaicin enhanced increases in soluble organics. All  
336 these facts confirmed that the presence of capsaicin improved rather than reduced solubilization, indicating  
337 that capsaicin may inhibit the bio-processes involved in anaerobic co-digestion.

338 Table 1 summarizes the experiment value and model-simulation value of inhibition of capsaicin on  
339 dextran, glucose, acetate and H<sub>2</sub>. It can be seen that the specific degradation rates of dextran, glucose, acetate,  
340 and hydrogen in the blank (i.e., 0 mg/L capsaicin) were respectively  $8.07 \pm 0.26$ ,  $7.00 \pm 0.30$ ,  $2.85 \pm 0.14$ , and  
341  $0.24 \pm 0.01$  mg/g VS·h, and these values were considered the original activities of microbes relevant to  
342 hydrolysis, acidogenesis, acetotrophic methanogenesis, and hydrogenotrophic methanogenesis, respectively.

343 When 50 mg/L capsaicin was added, these values decreased respectively to  $6.19 \pm 0.62$ ,  $3.30 \pm 0.66$ ,  $1.12 \pm$   
344  $0.03$ , and  $0.17 \pm 0.02$  mg/g VS·h. This suggests 50 mg/L capsaicin reduced the relative activities of  
345 microbes (expressed as % of the original) relevant to hydrolysis, acidogenesis, acetotrophic methanogenesis,  
346 and hydrogenotrophic methanogenesis by 23%, 27%, 61%, and 29%, respectively. Similar observations  
347 were also made at 30 mg/L capsaicin.

348 From Table 1, it was also found that inhibition constant ( $K_{s,i}$ ) of capsaicin to the degradation of these  
349 substrates was in the order of acetate > H<sub>2</sub> > glucose > dextran, suggesting that the inhibition of capsaicin to  
350 these bioprocesses was in the sequence of acetotrophic methanogenesis > hydrogenotrophic methanogenesis >  
351 acidogenesis > hydrolysis. All the results showed that although capsaicin enhanced solubilization, it  
352 significantly inhibited the bioprocesses of hydrolysis, acidogenesis, and methanogenesis, especially  
353 acetotrophic methanogenesis. It can be understood why capsaicin inhibited methane production from  
354 anaerobic co-digestion.

355 It was reported that capsaicin could induce apoptosis by either altering key kinases (Pramanik and  
356 Srivastava 2012), or decreasing the intracellular NAD<sup>+</sup>/NADH ratio by binding to quinone binding site of  
357 NADH dehydrogenase 1 (NDH-1) (Lee et al. 2015b, Yagi 1990). Furthermore, Torrecillas et al. (2015)  
358 found capsaicin molecule could establish a molecular interaction with cell membrane, where the nine-carbon  
359 alkyl chain of capsaicin was aligned with the phospholipid acyl chains, perturbing the cooperative behavior of  
360 the phospholipid and inducing apoptosis. When capsaicin entered into the anaerobic co-digestion systems, it  
361 could contact with the membrane and key enzymes of anaerobes, or even enter into the intracellular cells.  
362 These behaviors may result in inactivation of functional enzymes, reduction in conversion between NAD<sup>+</sup> and  
363 NADH, or even cell lysis (Fig. 7A).

364 This deduction can be supported by flow cytometry, which is usually used to reflect the cell functional  
365 state. The physiological status of microorganism cells can be divided into four regions. Among them,  
366 viable cells are shown in AV<sup>-</sup>/PI (Q<sub>4</sub>), early apoptotic cells are shown in AV<sup>+</sup>/PI (Q<sub>3</sub>), necrotic (or late  
367 apoptotic) cells are shown in AV<sup>+</sup>/PI<sup>+</sup> (Q<sub>2</sub>), and debris and damaged cells are shown in AV<sup>-</sup>/PI<sup>+</sup> (Q<sub>1</sub>). It can be  
368 seen that with an increase of capsaicin from 0 to 50 mg/L the fluorescence percentage of viable cells  
369 decreased from 96.7% to 78.7%, while the fluorescence percentage of early apoptotic cells increased from 0.9%  
370 to 16.0% (Fig. 7B). This is the major reason for capsaicin enhancing solubilization but reducing hydrolysis,  
371 acidogenesis and methanogenesis.

372 According to the data shown in Table 1, it can be found that the inhibition of capsaicin to acetotrophic  
373 methanogenesis, one major pathway responsible for methane production, was much severer than that to  
374 hydrogenotrophic methanogenesis, the other methane production pathway. Thus, one might want to know  
375 why capsaicin caused different inhibitions to these two methane production pathways. In acetotrophic  
376 methanogenesis, acetate can be either converted into acetyl-phosphate and acetyl-CoA catalyzed by AK and  
377 PTA in turn or directly degraded to acetyl-CoA catalyzed by CoA. The generated acetyl-CoA is then  
378 converted into 5-methyl-THMPT under the catalysis of ACDS. In hydrogenotrophic methanogenesis, H<sub>2</sub> and  
379 CO<sub>2</sub> can be converted into 5-methyl-THMPT, with mch and F<sub>420</sub> being as the key enzymes (Fig. 8A). As the  
380 same intermediate in the two pathways, 5-methyl-THMPT then undergoes the succession steps of  
381 5-methyl-THMPT → methyl-CoM → CH<sub>4</sub>. It was found that although the presence of capsaicin inhibited  
382 the activity of all these enzymes in acetotrophic and hydrogenotrophic methanogenesis, its inhibition to CoA  
383 and ACDS was much severer than that to others (Fig. 8B). This may explain why capsaicin caused severer  
384 inhibition to acetotrophic methanogenesis than hydrogenotrophic methanogenesis.

385 When ACDS catalyzes the step of acetyl-CoA to 5-Methyl-THMPT, two electrons would be generated  
386 (Grahame and DeMoll 1996). In anaerobic digestion, the generated electrons are generally transferred to  
387 ferredoxin by 4Fe-4S clusters ligands on ACDS (Ferry 2011). Previous publication demonstrated that  
388 capsaicin could be activated to an electrophilic intermediate, and this intermediate could compete for the  
389 electrons available for ferredoxin utilization (Fig. 8C) (Surh and Lee 1995). This causes reductions in the  
390 electrons transferred by 4Fe-4S clusters ligands on ACDS, which might be the reason for capsaicin severely  
391 inhibiting the activity of ACDS. Moreover, it is reported that the amino group of capsaicin can be subjected  
392 to dehydration condensation reaction with carboxyl group of CoA, inhibiting the metabolic activity of CoA  
393 (Yue et al. 2020).

### 394 3.6 Effect of capsaicin on microbial community.

395 Illumina Miseq 16S-rRNA genes sequencing was performed to investigate the effect of capsaicin on  
396 microbial community by comparing the structure and abundance of microbial community between the control  
397 and experimental reactors. The control reactor was fed with 2 mg/g VS capsaicin co-substrates, while the  
398 experimental reactor was fed with 68 mg/g VS capsaicin co-substrates. The number of operational  
399 taxonomic units was 1074 in the control reactor and 1050 in the experimental digester, with 886 being shared  
400 (Fig. S5). The Alpha diversity results (Table S2) showed that PD index was similar in the two reactors,  
401 while Chao index in the control was greater than that in the experiment reactor, suggesting that the increase of  
402 capsaicin reduced the microbial diversity but did not change largely the microbial structure.

403 At the phylum level, the most predominant bacteria in the two reactors were *Firmicutes*, *Bacteroidetes*,  
404 *Proteobacteria*, and *Actinobacteria* (Fig. S6). It is reported that several anaerobes in these phyla can degrade  
405 organic compounds (e.g., proteins and carbohydrates) (Wei et al. 2019), and many bacteria affiliated to  
406 *Firmicutes* and *Proteobacteria* were volatile fatty acid producers (Wang et al. 2017). *Euryarchaeota* was the

407 only archaeal phylum in the two reactors (Fig. S6), which was known as methanogens and detected in several  
408 anaerobic digesters (Wei et al. 2019).

409 Fig. 9 displays the genus-level distributions of bacteria and archaea abundances in the two reactors.  
410 Seven genera of bacteria, which were responsible for hydrolysis and acidogenesis, were detected in the two  
411 reactors. For example, the abundance of *Bacteroides*, which was reported to degrade carbohydrates and  
412 organic acids (Pang et al. 2020), was measured to be 17.6% in the control, but it was completely washed out  
413 in the experiment reactor. The abundances of *Dysgonomonadaceae*, *Petrimonas*, and *Macellibacteroides*,  
414 which were able to degrade various polysaccharides and proteins (Maspolim et al. 2015, Murakami et al. 2018,  
415 Xu et al. 2019), reduced from 6.5%, 5.3%, and 7.9% in the control to 3.2%, 2.4%, and 1.2% in the experiment  
416 reactor, respectively (Fig. 9A). Further calculation showed that the total abundance of these genera was 42.6%  
417 in the control and 14.8% in the experiment reactor, indicating that capsaicin reduced largely the number of  
418 anaerobes relevant to hydrolysis and acidogenesis.

419 It can be also seen from Fig. 9A that the abundance of *Escherichia-Shigella*, a resistant genus having  
420 ability to degrade aromatic organic pollutants (Cui et al. 2017, Vasiliadou et al. 2018), increased from 1.0% in  
421 the control to 10.7% in the experiment reactor. Moreover, the abundance of several other contaminant  
422 degradation microbes such as *Fonticella*, *Pirellulaceae*, *Enterococcus* and *Herbinix* (Cao et al. 2018, Fraj et al.  
423 2013, Koeck et al. 2016, Tong et al. 2017), increased with capsaicin addition as well. The total abundance of  
424 potential complex organic degradation microbes increased from 20.7% in the control to 42.4% in the  
425 experiment reactor, suggesting that these microbes might be capsaicin decomposers in such anaerobic  
426 co-digestion systems.

427 Fig. 9B shows the distribution of archaea community in the two reactors. The total sequences of  
428 methanogens decreased from 16313 in the control to 7592 in the experiment reactor, suggested that the

429 addition of capsaicin reduced the total archaea populations. Among them, the abundance of  
430 *Methanobacterium*, decreased from 73.4% in the control to 64.7% in the experiment reactor. However, the  
431 abundances of *Methanobrevibacter* and *Methanosphaera* increased from 2.0% and 0.2% in the control to 9.1%  
432 and 2.2%, respectively. This suggest that the effect of capsaicin on different types of archaea is different,  
433 and manipulation of co-digesters to enrich *Methanobrevibacter* and *Methanosphaera* could effectively  
434 mitigate the inhibition of capsaicin to methane production. The accurate reason for this different impact is  
435 unclear at the current stage, more efforts are required in the future.

#### 436 **4. Conclusions**

437 This study evaluated the degradation of capsaicin in anaerobic co-digestion of FW and WAS and  
438 explored the effect of capsaicin on methane production as well as the underlying mechanisms of capsaicin  
439 affecting methane yield. The findings obtained not only advance the understanding of capsaicin-involved  
440 digestion but also guide engineers to develop effective strategies in the future to manipulate anaerobic  
441 co-digestion of FW and WAS. The main conclusions are:

442 (1) Capsaicin can be degraded by some microbe and used as substrate to produce methane.

443 HPLC-MS/MS analysis that hydroxylation, O-demethylation, dehydrogenation and doubly  
444 oxidization are involved in capsaicin degradation.

445 (2) The presence of capsaicin not only slowed the process of anaerobic co-digestion but also decreased  
446 methane yield. With the increase of capsaicin from  $2 \pm 0.7$  to  $68 \pm 4$  mg/g VS, the maximal methane  
447 yield decreased from  $274.6 \pm 9.7$  to  $188.9 \pm 8.4$  mL/g VS, while the methane production rate  
448 decreased from 17.76 to 6.63 mL/(g VS·d).

449 (3) Mechanism investigations revealed that the presence of capsaicin induced apoptosis, which led to  
450 significant inhibitions to hydrolysis, acidogenesis, and methanogenesis, especially acetotrophic  
451 methanogenesis.

452 (4) The presence of capsaicin enhanced the populations of complex organic degradation microbes such  
453 as *Escherichia-Shigella* and *Fonticella* but decreased the numbers of anaerobes relevant to hydrolysis,  
454 acidogenesis, and methanogenesis such as *Bacteroide* and *Methanobacterium*.

#### 455 **Acknowledgements**

456 This study was financially supported by the Natural Science Funds of Hunan Province for Distinguished  
457 Young Scholar (2018JJ1002)

#### 458 **Appendix A. Supplementary data**

459 This file contains Text S1-S3, Table S1-S2 and Fig. S1-S6.

460

461 **References**

- 462 Cao, J., Wang, C., Dou, Z., Liu, M. and Ji, D. (2018) Hyphospheric impacts of earthworms and arbuscular mycorrhizal fungus on soil  
463 bacterial community to promote oxytetracycline degradation. *J. Hazard. Mater.* 341, 346-354.
- 464 Cho, S., Moon, H.-I., Hong, G.-E., Lee, C.-H., Kim, J.-M. and Kim, S.-K. (2014) Biodegradation of capsaicin by *Bacillus*  
465 *licheniformis* SK1230. *J. Korean. Soc. Appl. Bi.* 57(3), 335-339.
- 466 Cui, D., Shen, D., Wu, C., Li, C., Leng, D. and Zhao, M. (2017) Biodegradation of aniline by a novel bacterial mixed culture *AC*. *Int.*  
467 *Biodeter. Biodegr.* 125, 86-96.
- 468 Ferry, J.G. (2011) Fundamentals of methanogenic pathways that are key to the biomethanation of complex biomass. *Curr. Opin.*  
469 *Biotechnol.* 22(3), 351-357.
- 470 Fraj, B., Ben Hania, W., Postec, A., Hamdi, M., Ollivier, B. and Fardeau, M.-L. (2013) *Fonticella tunisiensis* gen. nov., sp. nov.,  
471 isolated from a hot spring. *Int. J. Evol. Microbiol.* 63(Pt\_6), 1947-1950.
- 472 Gonzalez-Gil, L., Krah, D., Ghattas, A.K., Carballa, M., Wick, A., Helmholz, L., Lema, J.M. and Ternes, T.A. (2019)  
473 Biotransformation of organic micropollutants by anaerobic sludge enzymes. *Water Res.* 152, 202-214.
- 474 Grahame, D.A. and DeMoll, E. (1996) Partial reactions catalyzed by protein components of the acetyl-CoA decarbonylase synthase  
475 enzyme complex from *Methanosarcina barkeri*. *J. Biol. Chem.* 271(14), 8352-8358.
- 476 Gu, H., Yang, Z., Yu, W., Xu, K. and Fu, Y.-f. (2019) Antibacterial Activity of Capsaicin against Sectional Cariogenic Bacteria. *Pak. J.*  
477 *Zool.* 51(2).
- 478 Huang, X., Liu, X., Chen, F., Wang, Y., Li, X., Wang, D., Tao, Z., Xu, D., Xue, W., Geng, M. and Yang, Q. (2020) Clarithromycin  
479 affect methane production from anaerobic digestion of waste activated sludge. *J. Clean. Prod.* 255, 120321.
- 480 Hwang, I.M., Choi, J.Y., Nho, E.Y., Lee, G.H., Jamila, N., Khan, N., Jo, C.H. and Kim, K.S. (2017) Characterization of Red Peppers  
481 (*Capsicum annuum*) by High-performance Liquid Chromatography and Near-infrared Spectroscopy. *Anal. Lett.* 50(13),  
482 2090-2104.
- 483 Jia, Y., Khanal, S.K., Shu, H., Zhang, H., Chen, G.H. and Lu, H. (2018) Ciprofloxacin degradation in anaerobic sulfate-reducing  
484 bacteria (SRB) sludge system: Mechanism and pathways. *Water Res.* 136, 64-74.
- 485 Koeck, D.E., Hahnke, S., Zverlov, V.V. and Zverlov, V.V. (2016) *Herbinix luporum* sp. nov., a thermophilic cellulose-degrading  
486 bacterium isolated from a thermophilic biogas reactor. *Int. J. Syst. Evol. Microbiol.* 66(10), 4132-4137.
- 487 Kurita, S., Kitagawa, E., Kim, C.H., Momose, Y. and Iwahashi, H. (2002) Studies on the antimicrobial mechanisms of capsaicin using  
488 yeast DNA microarray. *Biosci. Biotechnol. Biochem.* 66(3), 532-536.
- 489 López-Carrillo, L.; Hernández Avila, M. and Dubrow, R. (1994) Chili pepper consumption and gastric cancer in Mexico: a

490 case-control study. *Am. Epidemiol.* 139(3), 263-271.

491 Lay, J.-J., Li, Y.-Y. and Noike, T. (1997) Influences of pH and moisture content on the methane production in high-solids sludge  
492 digestion. *Water Res.* 31(6), 1518-1524.

493 Lee, M., Cho, J.-Y., Lee, Y.G., Lee, H.J., Lim, S.-I., Park, S.-L. and Moon, J.-H. (2015a) Bioconversion of Capsaicin by *Aspergillus*  
494 *oryzae*. *J. Agr. Food. Chem.* 63(26), 6102-6108.

495 Lee, Y.-H., Chen, H.-Y., Su, L.J. and Chueh, P.J. (2015b) Sirtuin 1 (SIRT1) Deacetylase Activity and NAD<sup>+</sup>/NADH Ratio Are  
496 Imperative for Capsaicin-Mediated Programmed Cell Death. *J. Agr. Food. Chem.* 63(33), 7361-7370.

497 Li, Y., Xu, Q., Liu, X., Wang, Y., Wang, D., Yang, G., Yuan, X., Yang, F., Huang, J. and Wu, Z. (2020a) Peroxide/Zero-valent iron (Fe<sup>0</sup>)  
498 pretreatment for promoting dewaterability of anaerobically digested sludge: A mechanistic study. *Journal of Hazardous Materials*  
499 400, 123112.

500 Li, Y., Zhu, Y., Wang, D., Yang, G., Pan, L., Wang, Q., Ni, B.-J., Li, H., Yuan, X., Jiang, L. and Tang, W. (2020b) Fe(II) catalyzing  
501 sodium percarbonate facilitates the dewaterability of waste activated sludge: Performance, mechanism, and implication. *Water*  
502 *Research* 174, 115626.

503 Li, X., Chen, Y., Zhao, S., Chen, H., Zheng, X., Luo, J. and Liu, Y. (2015) Efficient production of optically pure L-lactic acid from  
504 food waste at ambient temperature by regulating key enzyme activity. *Water Res.* 70, 148-157.

505 Li, Y., Jin, Y., Li, J., Li, H. and Yu, Z. (2016) Effects of pungency degree on mesophilic anaerobic digestion of kitchen waste. *Appl.*  
506 *Energ.* 181, 171-178.

507 Liu, K., Chen, Y., Xiao, N., Zheng, X. and Li, M. (2015) Effect of humic acids with different characteristics on fermentative  
508 short-chain fatty acids production from waste activated sludge. *Environ. Sci. Technol.* 49(8), 4929-4936.

509 Liu, X., Du, M., Yang, J., Wu, Y., Xu, Q., Wang, D., Yang, Q., Yang, G. and Li, X. (2020a) Sulfite serving as a pretreatment method for  
510 alkaline fermentation to enhance short-chain fatty acid production from waste activated sludge. *Chem. Eng. J.* 385.

511 Liu, X., Huang, X., Wu, Y., Xu, Q., Du, M., Wang, D., Yang, Q., Liu, Y., Ni, B.-J., Yang, G., Yang, F. and Wang, Q. (2020b) Activation  
512 of nitrite by freezing process for anaerobic digestion enhancement of waste activated sludge: Performance and mechanisms.  
513 *Chemical Engineering Journal* 387, 124147.

514 Liu, X., Xu, Q., Wang, D., Wu, Y., Yang, Q., Liu, Y., Wang, Q., Li, X., Li, H., Zeng, G. and Yang, G. (2019) Unveiling the mechanisms  
515 of how cationic polyacrylamide affects short-chain fatty acids accumulation during long-term anaerobic fermentation of waste  
516 activated sludge. *Water Res.* 155, 142-151.

517 Luo, J., Chen, Y. and Feng, L. (2016) Polycyclic Aromatic Hydrocarbon Affects Acetic Acid Production during Anaerobic  
518 Fermentation of Waste Activated Sludge by Altering Activity and Viability of Acetogen. *Environ. Sci. Technol.* 50(13),  
519 6921-6929.

520 Luo, J., Huang, W., Guo, W., Ge, R., Zhang, Q., Fang, F., Feng, Q., Cao, J. and Wu, Y. (2020a) Novel strategy to stimulate the food  
521 wastes anaerobic fermentation performance by eggshell wastes conditioning and the underlying mechanisms. *Chemical*  
522 *Engineering Journal* 398, 125560.

523 Luo, J., Zhang, Q., Zhao, J., Wu, Y., Wu, L., Li, H., Tang, M., Sun, Y., Guo, W., Feng, Q., Cao, J. and Wang, D. (2020b) Potential  
524 influences of exogenous pollutants occurred in waste activated sludge on anaerobic digestion: A review. *J. Hazard. Mater.* 383,  
525 121176.

526 Maspolim, Y., Zhou, Y., Guo, C., Xiao, K. and Ng, W.J. (2015) The effect of pH on solubilization of organic matter and microbial  
527 community structures in sludge fermentation. *Bioresour. Technol.* 190, 289-298.

528 Mehariya, S., Patel, A.K., Obulisamy, P.K., Punniyakotti, E. and Wong, J.W.C. (2018) Co-digestion of food waste and sewage sludge  
529 for methane production: Current status and perspective. *Bioresour. Technol.* 265, 519-531.

530 Monsereenusorn, Y. (1983) Subchronic toxicity studies of capsaicin and capsicum in rats. *Res. Commun. Chem. Pathol. Pharmacol.*  
531 41(1), 95-110.

532 Murakami, T., Segawa, T., Takeuchi, N., Barcaza Sepulveda, G., Labarca, P., Kohshima, S. and Hongoh, Y. (2018) Metagenomic  
533 analyses highlight the symbiotic association between the glacier stonefly *Andiperla willinki* and its bacterial gut community.  
534 *Environ. Microbiol.* 20(11), 4170-4183.

535 Nghiem, L.D., Koch, K., Bolzonella, D. and Drewes, J.E. (2017) Full scale co-digestion of wastewater sludge and food waste:  
536 Bottlenecks and possibilities. *Renew. Sust. Energ. Rev.* 72, 354-362.

537 Pang, H., Ma, W., He, J., Pan, X., Ma, Y., Guo, D., Yan, Z. and Nan, J. (2020) Hydrolase activity and microbial community dynamic  
538 shift related to the lack in multivalent cations during cation exchange resin-enhanced anaerobic fermentation of waste activated  
539 sludge. *J. Hazard. Mater.* 398, 122930.

540 Parrish, M.J.J.o.A.I. (1996) Liquid Chromatographic Method for Determining Capsaicinoids in Capsicums and Their Extractives:  
541 Collaborative Study. *J. Aoac. Int.* 79(3), 738-745.

542 Pramanik, K.C. and Srivastava, S.K. (2012) Apoptosis Signal-Regulating Kinase 1 $\Gamma$ Thioredoxin Complex Dissociation by  
543 Capsaicin Causes Pancreatic Tumor Growth Suppression by Inducing Apoptosis. *Antioxid. Redox. Sign.* 17(10), 1417-1432.

544 Reilly, C.A., Ehlhardt, W.J., Jackson, D.A., Kulanthaivel, P., Mutlib, A.E., Espina, R.J., Moody, D.E., Crouch, D.J. and Yost, G.S.  
545 (2003) Metabolism of capsaicin by cytochrome P450 produces novel dehydrogenated metabolites and decreases cytotoxicity to  
546 lung and liver cells. *Chem. Res. Toxicol.* 16(3), 336-349.

547 Reilly, C.A. and Yost, G.S. (2006) Metabolism of Capsaicinoids by P450 Enzymes: A Review of Recent Findings on Reaction  
548 Mechanisms, Bio-Activation, and Detoxification Processes. *Drug Metab. Rev.* 38(4), 685-706.

549 Shah, A.G., Pierson, J.A. and Pavlostathis, S.G. (2005) Fate and effect of the antioxidant ethoxyquin on a mixed methanogenic culture.

550 Water Res. 39(17), 4251-4263.

551 Sole-Bundo, M., Eskicioglu, C., Garfi, M., Carrere, H. and Ferrer, I. (2017) Anaerobic co-digestion of microalgal biomass and wheat  
552 straw with and without thermo-alkaline pretreatment. *Bioresour. Technol.* 237, 89-98.

553 Surh, Y.J. and Lee, S.S. (1995) Capsaicin, a double-edged sword: toxicity, metabolism, and chemopreventive potential. *Life Sci.*  
554 56(22), 1845-1855.

555 Tao, Z., Wang, D., Yao, F., Huang, X., Wu, Y., Du, M., Chen, Z., An, H., Li, X. and Yang, Q. (2020) The effects of thiosulfates on  
556 methane production from anaerobic co-digestion of waste activated sludge and food waste and mitigate method. *J Hazard Mater*  
557 384, 121363.

558 Tian, K., Zhu, J., Li, M. and Qiu, X. (2019) Capsaicin is efficiently transformed by multiple cytochrome P450s from *Capsicum*  
559 fruit-feeding *Helicoverpa armigera*. *Pestic. Biochem. Physiol.* 156, 145-151.

560 Tong, J., Lu, X., Zhang, J., Sui, Q., Wang, R., Chen, M. and Wei, Y. (2017) Occurrence of antibiotic resistance genes and mobile  
561 genetic elements in enterococci and genomic DNA during anaerobic digestion of pharmaceutical waste sludge with different  
562 pretreatments. *Bioresour. Technol.* 235, 316-324.

563 Torrecillas, A., Schneider, M., Fernandez-Martinez, A.M., Ausili, A., de Godos, A.M., Corbalan-Garcia, S. and Gomez-Fernandez, J.C.  
564 (2015) Capsaicin Fluidifies the Membrane and Localizes Itself near the Lipid-Water Interface. *ACS. Chem. Neurosci.* 6(10),  
565 1741-1750.

566 Vasiliadou, I.A., Molina, R., Martinez, F., Melero, J.A., Stathopoulou, P.M. and Tsiamis, G. (2018) Toxicity assessment of  
567 pharmaceutical compounds on mixed culture from activated sludge using respirometric technique: The role of microbial  
568 community structure. *Sci. Total. Environ.* 630, 809-819.

569 Wang, D., Duan, Y., Yang, Q., Liu, Y., Ni, B.J., Wang, Q., Zeng, G., Li, X. and Yuan, Z. (2018a) Free ammonia enhances dark  
570 fermentative hydrogen production from waste activated sludge. *Water Res.* 133, 272-281.

571 Wang, D., He, D., Liu, X., Xu, Q., Yang, Q., Li, X., Liu, Y., Wang, Q., Ni, B.J. and Li, H. (2019a) The underlying mechanism of  
572 calcium peroxide pretreatment enhancing methane production from anaerobic digestion of waste activated sludge. *Water Res.* 164,  
573 114934.

574 Wang, D., Liu, X., Zeng, G., Zhao, J., Liu, Y., Wang, Q., Chen, F., Li, X. and Yang, Q. (2018b) Understanding the impact of cationic  
575 polyacrylamide on anaerobic digestion of waste activated sludge. *Water Res.* 130, 281-290.

576 Wang, D., Zhao, J., Zeng, G., Chen, Y., Bond, P.L. and Li, X. (2015) How Does Poly(hydroxyalkanoate) Affect Methane Production  
577 from the Anaerobic Digestion of Waste-Activated Sludge? *Environ. Sci. Technol.* 49(20), 12253-12262.

578 Wang, J., Shi, T., Yang, X., Han, W. and Zhou, Y. (2014) Environmental risk assessment on capsaicin used as active substance for  
579 antifouling system on ships. *Chemosphere.* 104, 85-90.

580 Wang, Y., Wang, D., Chen, F., Yang, Q., Li, Y., Li, X. and Zeng, G. (2019b) Effect of triclocarban on hydrogen production from dark  
581 fermentation of waste activated sludge. *Bioresour. Technol.* 279, 307-316.

582 Wang, Y., Wang, D., Liu, Y., Wang, Q., Chen, F., Yang, Q., Li, X., Zeng, G. and Li, H. (2017) Triclocarban enhances short-chain fatty  
583 acids production from anaerobic fermentation of waste activated sludge. *Water Res.* 127, 150-161.

584 Wei, W., Huang, Q.S., Sun, J., Dai, X. and Ni, B.J. (2019) Revealing the Mechanisms of Polyethylene Microplastics Affecting  
585 Anaerobic Digestion of Waste Activated Sludge. *Environ. Sci. Technol.* 53(16), 9604-9613.

586 Wu, Y., Wang, D., Liu, X., Xu, Q., Chen, Y., Yang, Q., Li, H. and Ni, B. (2019) Effect of poly aluminum chloride on dark fermentative  
587 hydrogen accumulation from waste activated sludge. *Water Res.* 153, 217-228.

588 Xu, F., Li, Y., Ge, X., Yang, L. and Li, Y. (2018) Anaerobic digestion of food waste - Challenges and opportunities. *Bioresour Technol*  
589 247, 1047-1058.

590 Xu, Q., Li, X., Ding, R., Wang, D., Liu, Y., Wang, Q., Zhao, J., Chen, F., Zeng, G., Yang, Q. and Li, H. (2017) Understanding and  
591 mitigating the toxicity of cadmium to the anaerobic fermentation of waste activated sludge. *Water Res.* 124, 269-279.

592 Xu, Q., Liu, X., Wang, D., Liu, Y., Wang, Q., Ni, B.J., Li, X., Yang, Q. and Li, H. (2019) Enhanced short-chain fatty acids production  
593 from waste activated sludge by sophorolipid: Performance, mechanism, and implication. *Bioresour. Technol.* 284, 456-465.

594 Yagi, T. (1990) Inhibition by capsaicin of NADH-quinone oxidoreductases is correlated with the presence of energy-coupling site 1 in  
595 various organisms. *Arch. Biochem. Biophys.* 281(2), 305-311.

596 Yao, Z., Su, W., Wu, D., Tang, J., Wu, W., Liu, J. and Han, W. (2018) A state-of-the-art review of biohydrogen producing from sewage  
597 sludge. *Int. J. Energ. Res.* 42(14), 4301-4312.

598 Yue, L., Cheng, J., Zhang, H., Yuan, L., Hua, J., Dong, H., Li, Y.-y. and Zhou, J. (2020) Inhibition of N-Vanillylnonanamide in  
599 anaerobic digestion of lipids in food waste: Microorganisms damage and blocked electron transfer. *J. Hazard. Mater.* 399.

600 Zhang, C., Su, H., Baeyens, J. and Tan, T. (2014) Reviewing the anaerobic digestion of food waste for biogas production. *Renew. Sust.*  
601 *Energ. Rev.* 38, 383-392.

602 Zhang, J., Li, W., Lee, J., Loh, K.-C., Dai, Y. and Tong, Y.W. (2017) Enhancement of biogas production in anaerobic co-digestion of  
603 food waste and waste activated sludge by biological co-pretreatment. *Energy.* 137, 479-486.

604 Zhao, J., Zhang, C., Wang, D., Li, X., An, H., Xie, T., Chen, F., Xu, Q., Sun, Y., Zeng, G. and Yang, Q. (2016) Revealing the  
605 Underlying Mechanisms of How Sodium Chloride Affects Short-Chain Fatty Acid Production from the Cofermentation of Waste  
606 Activated Sludge and Food Waste. *ACS Sustain. Chem. Eng.* 4(9), 4675-4684.

607 Zhu, J., Tian, K., Reilly, C.A. and Qiu, X. (2020) Capsaicinoid metabolism by the generalist *Helicoverpa armigera* and specialist *H.*  
608 *assulta*: Species and tissue differences. *Pestic. Biochem. Physiol.* 163, 164-174.

609

610 **List of Table and Figures**

611 **Table 1.** Experiment and model values of capsaicin inhibition to dextran, glucose, acetate and H<sub>2</sub> conversions.

612 **Fig. 1.** Variations in HPLC chromatogram (A) and capsaicin concentration (B) at different digestion times.

613 **Fig. 2.** Full scan mode LC/MS chromatogram of capsaicin and metabolites produced in digestion process  
614 extracted samples withdrawn from the digester fed with  $68 \pm 4.1$  mg/g VS.

615 **Fig. 3.** Representative MS/MS spectra of M (A), M1 (B), M2 (C), and M3 (D). The structures and  
616 fragmentation patterns of key diagnostic ions are presented in the figure.

617 **Fig. 4.** The possible pathways of capsaicin biodegradation during anaerobic co-digestion. The pathways  
618 shown in dash line were not demonstrated in this work and proposed according to the literature (Cho et al.  
619 2014, Yue et al. 2020).

620 **Fig. 5.** Measured and simulated (using modified Gompertz equation) methane production from anaerobic  
621 co-digestion in the presence of capsaicin at different concentrations. Symbols represent experimental data  
622 and lines represent model fit. Error bars represent standard deviations of triplicate tests.

623 **Fig. 6.** The soluble proteins (a), soluble carbohydrates (b), and EEM spectra (c) of digestion liquid. Samples  
624 were collected on 2 d digestion. Error bars represent standard deviations of triplicate tests. The samples  
625 used to determine fluorescence EEM were diluted by 50 times.

626 **Fig. 7.** The schematic diagram of interaction between capsaicin molecule and cell membrane (A), and flow  
627 cytometric analysis of physiological status of microorganism cell (B). B-I: 0 mg/L capsaicin (The control)  
628 (A), B-II: 30 mg/L capsaicin (B), and B-III: 50 mg/L capsaicin.

629 **Fig. 8.** Metabolic pathways of acetotrophic and hydrogenotrophic methanogenesis (A), the impact of  
630 capsaicin on the relative activities of key enzymes involved in the two pathways (B), and schematic diagram  
631 of capsaicin inhibiting the activity of ACDS (C). THMPT: tetrahydromethanopterin; AK: acetate kinase;

632 PTA: phosphotransacetylase; ACDS: acetyl-CoA decarboxylase/synthase; mch: methenyl-THMPT

633 cyclohydrolase; CoM: coenzyme-M. Error bars represent standard deviations of triplicate tests.

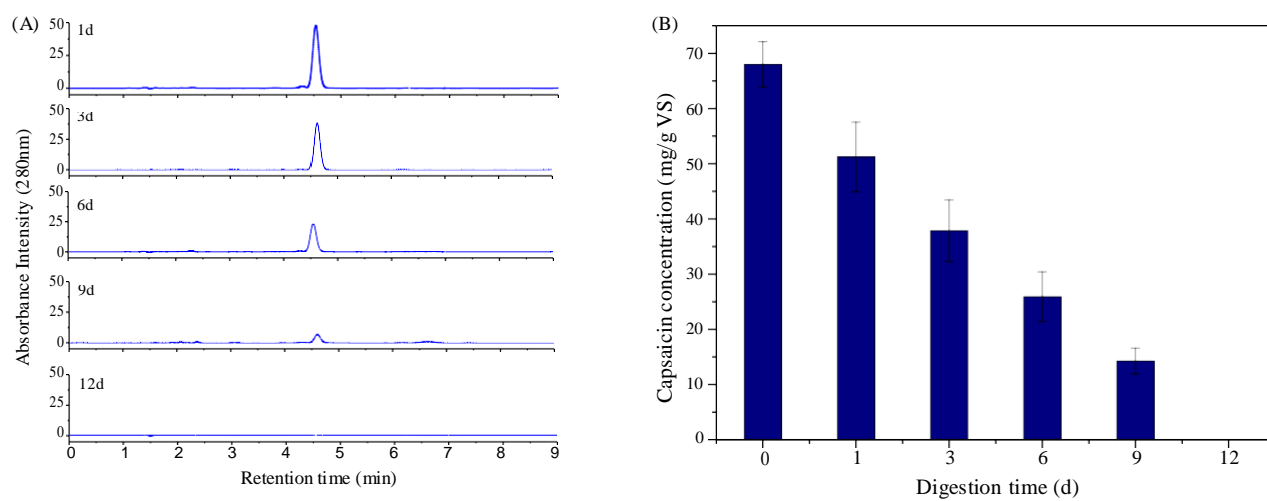
634 **Fig. 9.** The distribution of bacteria (A) and archaea (B) abundances at genus level in the two reactors.

**Table**[Click here to download Table: Table.docx](#)**1 Table 1**2 Experiment and model values of capsaicin inhibition to dextran, glucose, acetate and H<sub>2</sub> conversions.

Substrate	Experiment values <sup>a</sup>				Model values		
	0 mg/L	30mg/L	50 mg/L	X <sub>s,o</sub> <sup>b</sup>	X <sub>s,i</sub> <sup>c</sup>		K <sub>s,i</sub> <sup>d</sup>
					30 mg/L	50 mg/L	
Dextran	8.07±0.26	5.99±0.19	6.19±0.62	3.01	1.98	1.39	48.5
Glucose	7.00±0.30	5.56±0.35	5.12±0.66	2.00	1.41	1.05	35.9
Acetate	2.85±0.14	1.44±0.13	1.12±0.03	0.79	0.35	0.33	13.7
H <sub>2</sub>	0.24±0.01	0.19±0.02	0.17±0.02	1.90	1.45	1.34	33.4

3 <sup>a</sup> Results are the average and **their standard deviations of triplicate tests**, and the unit is mg/g VS·h4 <sup>b</sup> X<sub>s,o</sub> is the degradation of the substrate without capsaicin addition, and the unit is g/(L·d) or g/L.5 <sup>c</sup> X<sub>s,i</sub> is the degradation of the substrate when different capsaicin are added, and the unit is g/(L·d) or g/L.6 <sup>d</sup> K<sub>s,i</sub> is the related inhibition constant of capsaicin calculated by Eq (2), and the unit is mg/L.

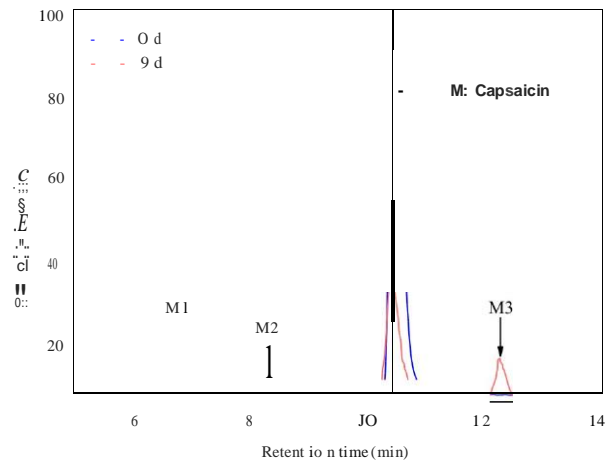
# Figure



1

2 **Fig. 1.** Variations in HPLC chromatogram (A) and capsaicin concentration (B) at different digestion times.

3

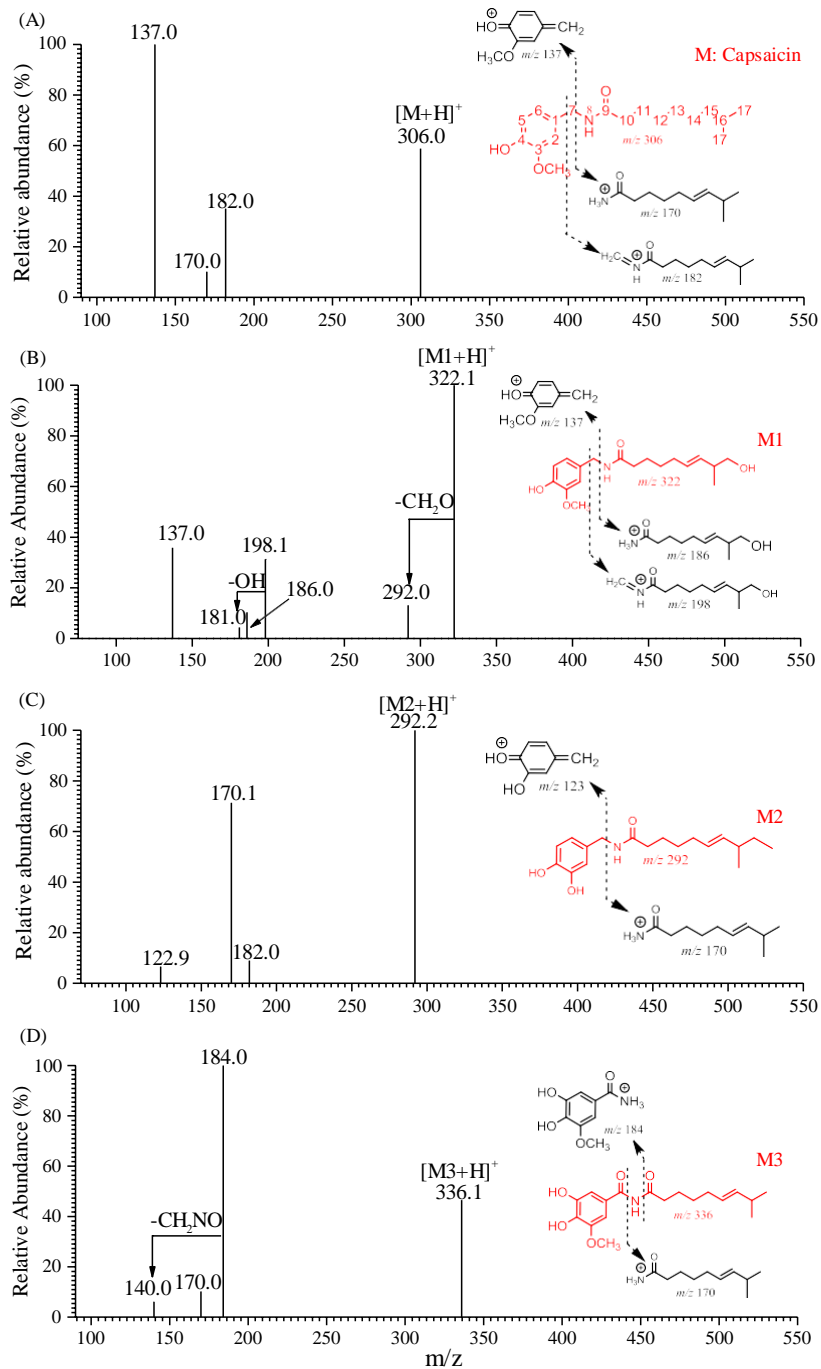


4

5 **Fig. 2.** Full scan mode LC/MS chromatogram of capsaicin and metabolites produced in digestion process

6 extracted samples withdrawn from the digester fed with  $68 \pm 4.1$  mg/g VS.

7

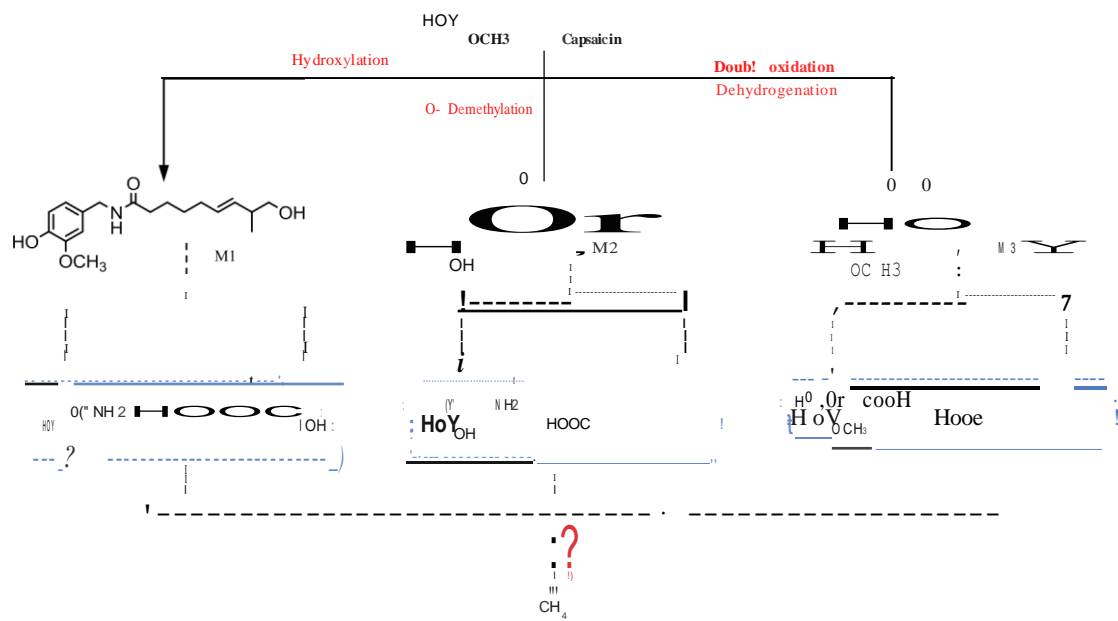


8

9 **Fig. 3.** Representative MS/MS spectra of M (A), M1 (B), M2 (C), and M3 (D). The structures and

10 fragmentation patterns of key diagnostic ions are presented in the figure.

11



12

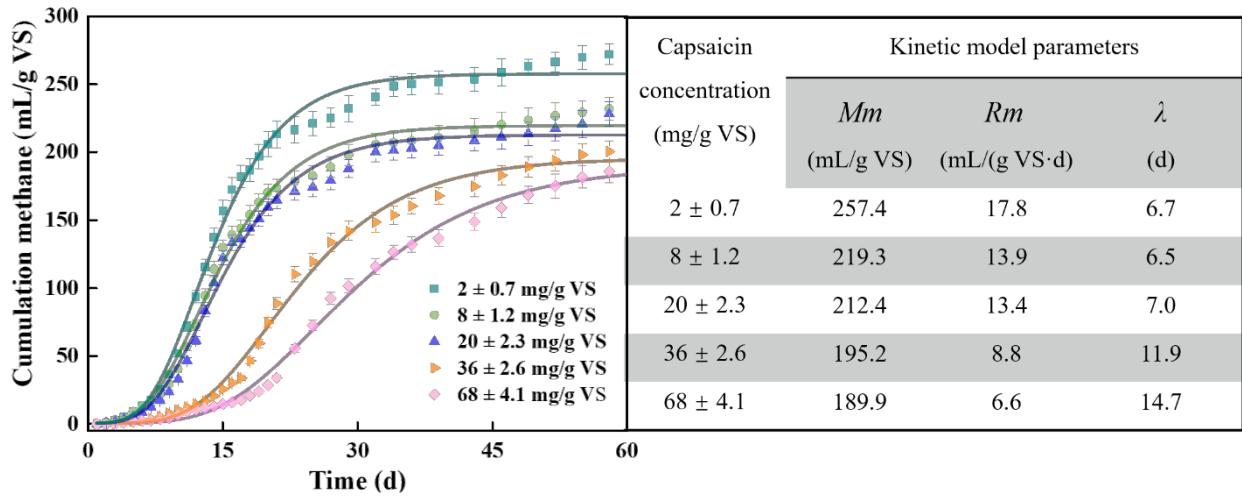
13

**Fig. 4.** The possible pathways of capsaicin biodegradation during anaerobic co-digestion. The pathways shown in dash line were not demonstrated in this work and proposed according to the literature (Cho et al. 2014, Yue et al. 2020).

14

15

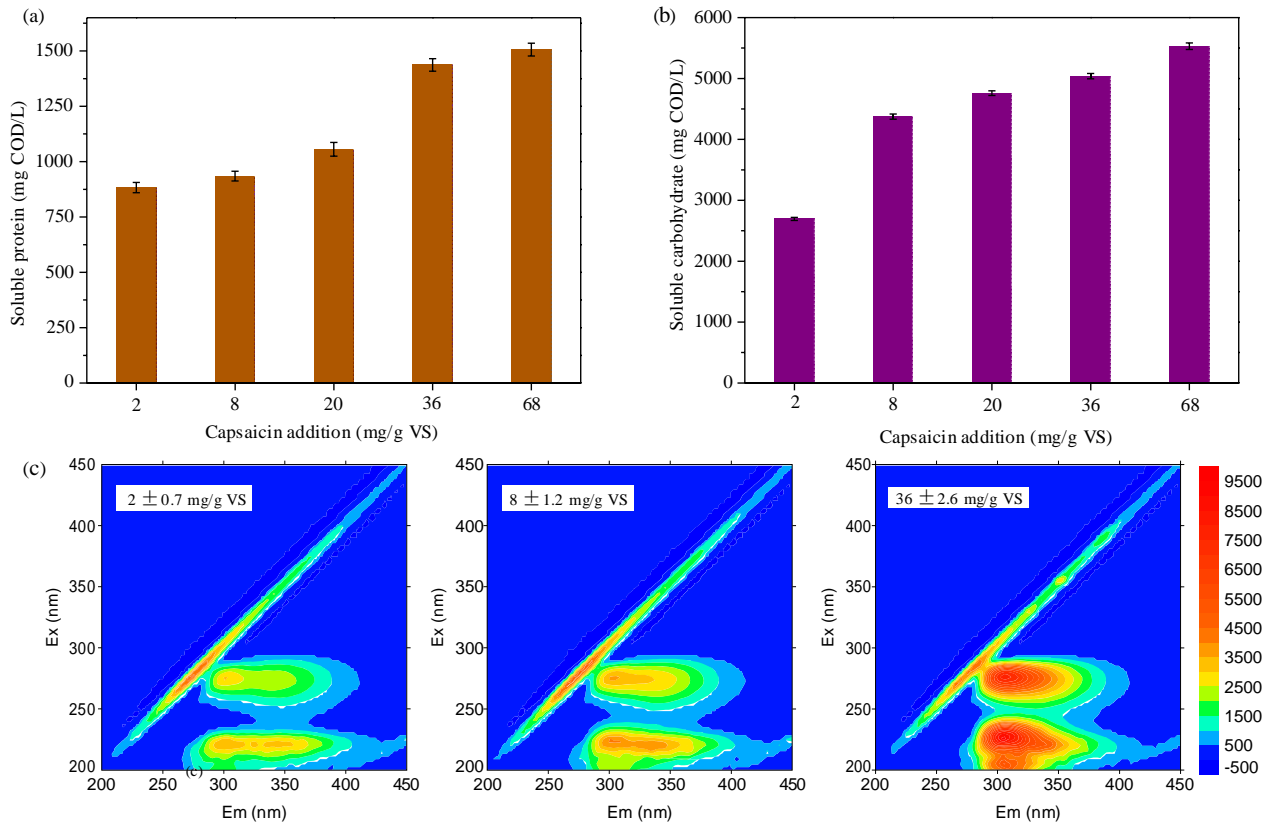
16



17

18 **Fig. 5.** Measured and simulated (using modified Gompertz equation) methane production from anaerobic  
 19 co-digestion in the presence of capsaicin at different concentrations. Symbols represent experimental data  
 20 and lines represent model fit. Error bars represent standard deviations of triplicate tests.

21



22

23

**Fig. 6.** The soluble proteins (a), soluble carbohydrates (b), and EEM spectra (c) of digestion liquid. Samples

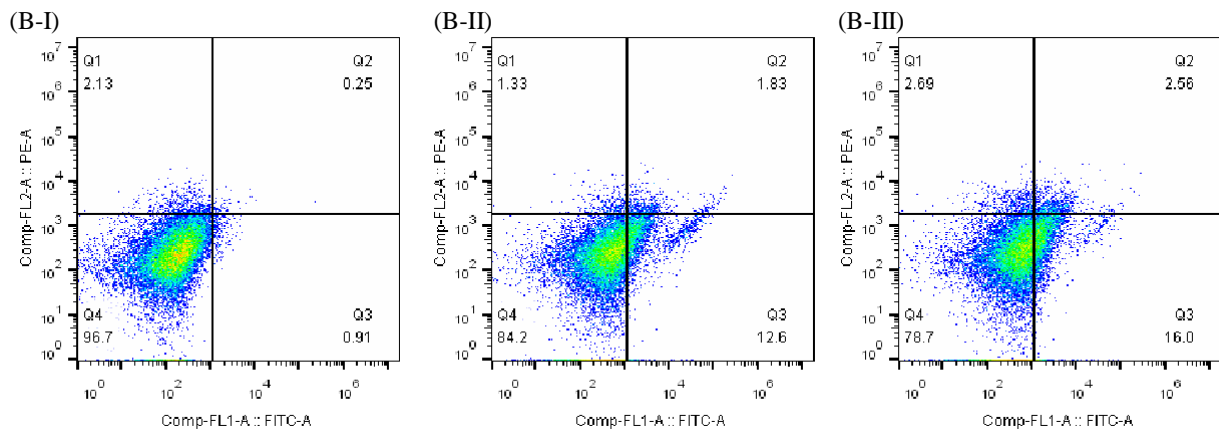
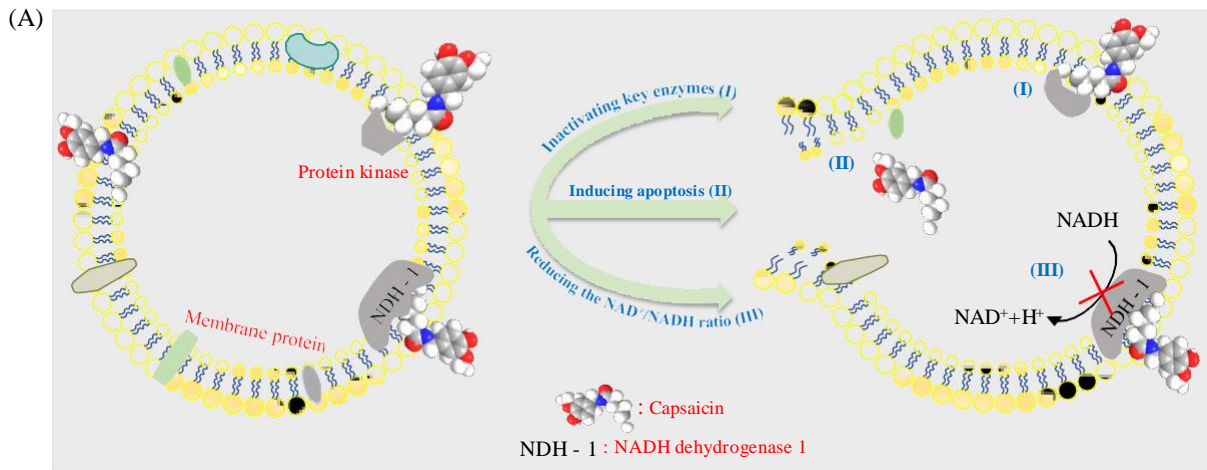
24

were collected on 2 d digestion. Error bars represent standard deviations of triplicate tests. The samples

25

used to determine fluorescence EEM were diluted by 50 times.

26



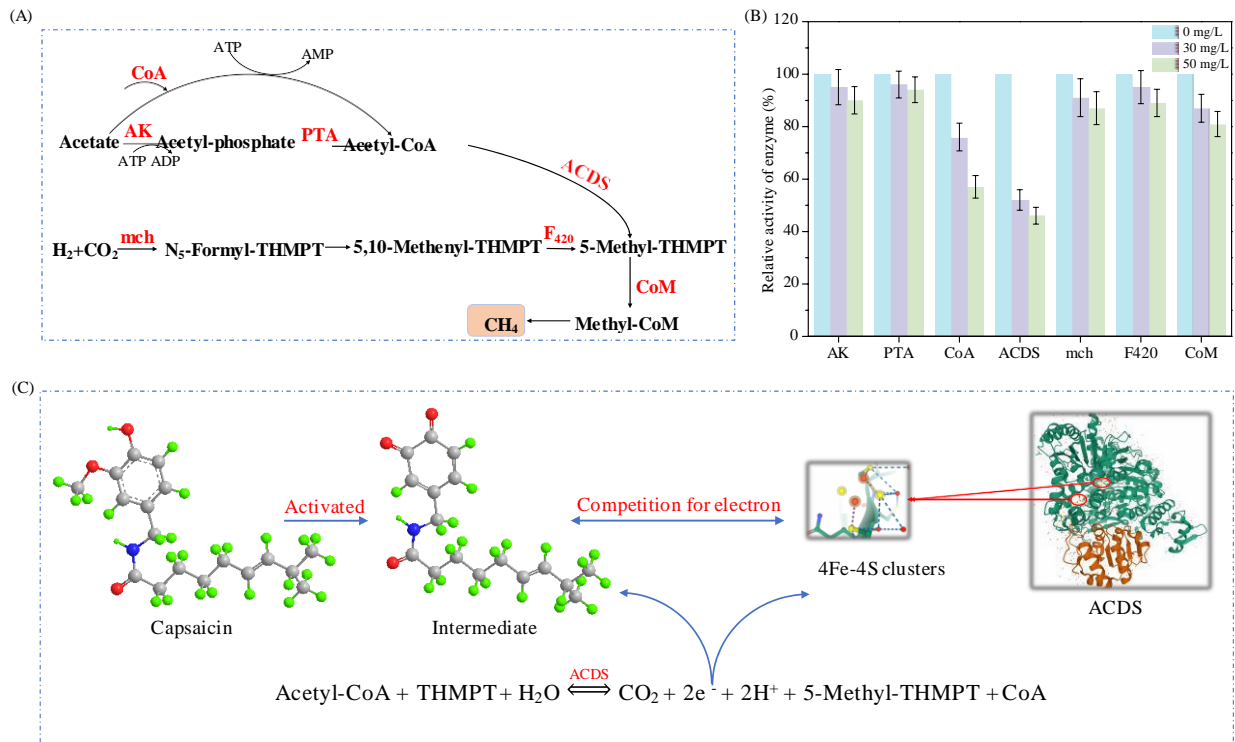
27

28 **Fig. 7.** The schematic diagram of interaction between capsaicin molecule and cell membrane (A), and flow

29 cytometric analysis of physiological status of microorganism cell (B). B-I: 0 mg/L capsaicin (The control)

30 (A), B-II: 30 mg/L capsaicin (B), and B-III: 50 mg/L capsaicin.

31



32

33 **Fig. 8.** Metabolic pathways of acetotrophic and hydrogenotrophic methanogenesis (A), the impact of capsaicin

34 on the relative activities of key enzymes involved in the two pathways (B), and schematic diagram of

35 capsaicin inhibiting the activity of ACDS (C). THMPT: tetrahydromethanopterin; AK: acetate kinase; PTA:

36 phosphotransacetylase; ACDS: acetyl-CoA decarbonylase/synthase; mch: methenyl-THMPT cyclohydrolase;

37 CoM: coenzyme-M. Error bars represent standard deviations of triplicate tests.

38



39

40 **Fig. 9.** The distribution of bacteria (A) and archaea (B) abundances at genus level in the two reactors.